LIC-Fusion 2.0: LiDAR-Inertial-Camera Odometry with Sliding-Window Plane-Feature Tracking

Xingxing Zuo[1,2], Yulin Yang[3], Patrick Geneva[3], Jiajun Lv[2]
Yong Liu[2], Guoquan Huang[3], Marc Pollefeys[1,4]

[1] ETH Zurich, Switzerland
[2] Zhejiang University, Hangzhou,China
[3] University of Delaware, USA
[4] Microsoft Mixed Reality and Artificial Intelligence Lab, Zurich Switzerland

Motivation

• 3D LiDAR, camera, inertial-measurement (IMU) have their inherent strengths and drawbacks.

• The data association for LiDAR sparse features is non-trivial and error-prone. How to address this issue in a non-iterative light-weight EKF[1]?

• How to make the estimator consistent and prevent the inconsistent-prone ICP for LiDAR scan matching?

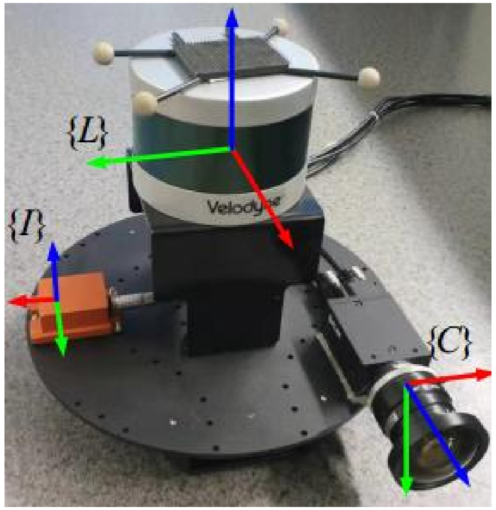

Fig. Sensor setup with a 3D LiDAR, IMU and a monocular camera.

[1] X. Zuo, P. Geneva, W. Lee, Y. Liu, and G. Huang. "LIC-Fusion: LiDAR-Inertial-Camera Odometry". In: Proc. IEEE/RSJ International Conference on Intelligent Robots and Systems (IROS). Nov. 2019, pp. 5848–5854.

System Overview

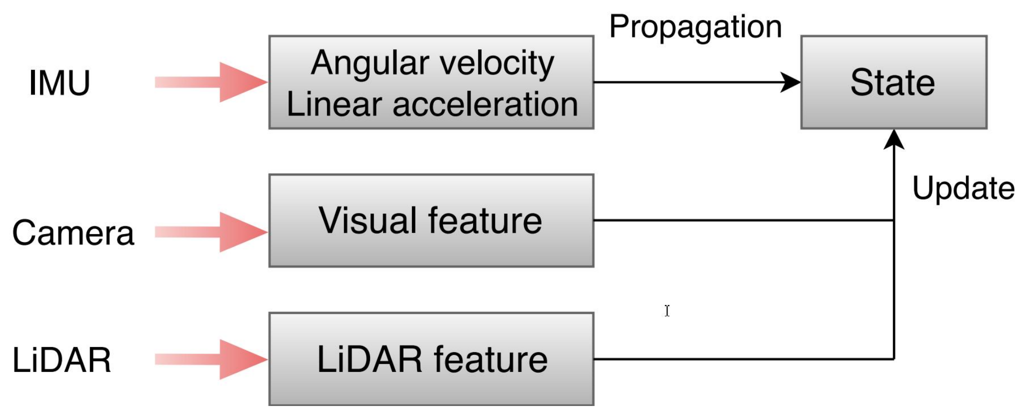

Fig. Data flow of LIC-fusion

- State vector include IMU states, extrinsics between sensors, cloned IMU poses at the time instants of receiving the images and LiDAR scans, point features and plane features:

$$\mathbf{x} = \begin{bmatrix} \mathbf{x}_I^\top & \mathbf{x}_{calib\_C}^\top & \mathbf{x}_{calib\_L}^\top & \mathbf{x}_C^\top & \mathbf{x}_L^\top & {}^G\mathbf{x}_f^\top & {}^A\mathbf{x}_\pi^\top \end{bmatrix}^\top$$

Update – Sparse LiDAR Feature

- Point ${}^{L}\mathbf{p}_f$ to plane ${}^{L}\mathbf{p}_\pi$ distance

$$\mathbf{z}_\pi = \frac{{}^{L}\mathbf{p}_\pi}{\left\|{}^{L}\mathbf{p}_\pi\right\|}\left({}^{L}\mathbf{p}_f - \mathbf{n}_f\right) - \left\|{}^{L}\mathbf{p}_\pi\right\|$$

Closet point to denote a 3D plane

$${}^{L}d = \left\|{}^{L}\mathbf{p}_\pi\right\|, {}^{L}\mathbf{n} = {}^{L}\mathbf{p}_\pi / \left\|{}^{L}\mathbf{p}_\pi\right\|$$

$$\begin{bmatrix} {}^{L}\mathbf{n} \\ {}^{L}d \end{bmatrix} = \begin{bmatrix} {}^{L}_{A}\mathbf{R} & 0 \\ -{}^{A}\mathbf{p}_L^\top & 1 \end{bmatrix} \begin{bmatrix} {}^{A}\mathbf{n} \\ {}^{A}d \end{bmatrix}$$

- Linearize the distance residual at current best estimated states

$$\mathbf{r}_f = \mathbf{0} - \mathbf{z}_f \simeq \mathbf{H}_x \tilde{\mathbf{x}} + \mathbf{H}_\pi {}^{A}\tilde{\mathbf{p}}_\pi + \mathbf{H}_n \mathbf{n}_f$$

Marginalize plane feature by the left nullspace N,

$$\mathbf{N}^\top \mathbf{r}_f = \mathbf{N}^\top \mathbf{H}_x \tilde{\mathbf{x}} + \mathbf{N}^\top \mathbf{H}_\pi {}^{A}\tilde{\mathbf{p}}_\pi + \mathbf{N}^\top \mathbf{H}_n \mathbf{n}_f$$

$$\Rightarrow \mathbf{r}_{fo} = \mathbf{H}_{xo} \tilde{\mathbf{x}} + \mathbf{n}_o$$

Due to the special structure that

$$\mathbf{H}_n \mathbf{H}_n^T = \mathbf{I}_n$$

the measurement covariance is still isotropic, thus the null space operation is still valid.

Sparse LiDAR Feature Tracking

- Track the planar LiDAR feature across frames (from green frame to red frame)

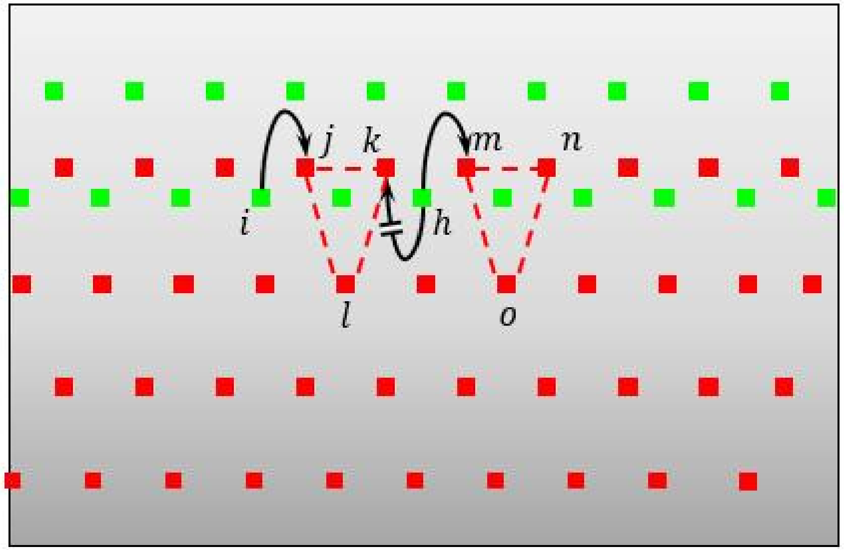

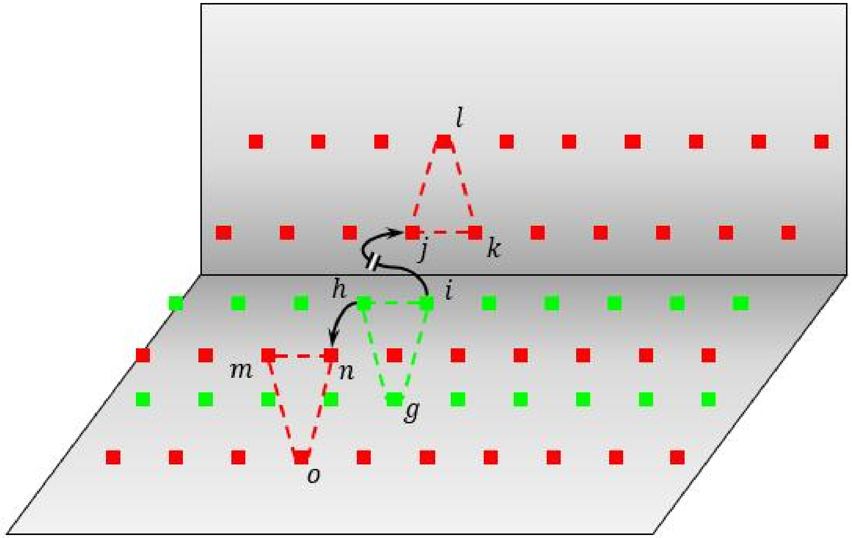

A point is associated with its closet triangle[1]. Meanwhile, make sure to prevent reusing information.

Tracking based on distance only is not enough!

[1] J. Zhang, S. Singh, LOAM: Lidar Odometry and Mapping in Real-time[C], Robotics: Science and Systems. 2014, 2: 9.

Sparse LiDAR Feature Tracking

- Normal vector based probabilistic planar feature data association

Measure the difference between two normal vectors derived from points $\left\{ {}^{L_a}\mathbf{p}_{fm} \quad {}^{L_a}\mathbf{p}_{fn} \quad {}^{L_a}\mathbf{p}_{fo} \right\}$ and points $\left\{ {}^{L_a}\mathbf{p}_{fh} \quad {}^{L_a}\mathbf{p}_{fi} \quad {}^{L_a}\mathbf{p}_{fg} \right\}$ respectively while taking into account the noises from relative pose.

$$\mathbf{z}_n = \left\lfloor {}^{L_a}\mathbf{n}_1 \right\rfloor_{L_b}^{L_a} \mathbf{R}\, {}^{L_b}\mathbf{n}_2$$

$${}^{L_a}\mathbf{n}_1 = \left\lfloor {}^{L_a}\mathbf{p}_{fn} - {}^{L_a}\mathbf{p}_{fm} \right\rfloor \left({}^{L_a}\mathbf{p}_{fo} - {}^{La}\mathbf{p}_{fm} \right)$$

$${}^{L_b}\mathbf{n}_2 = \left\lfloor {}^{L_b}\mathbf{p}_{fh} - {}^{L_b}\mathbf{p}_{fg} \right\rfloor \left({}^{L_b}\mathbf{p}_{fi} - {}^{L_b}\mathbf{p}_{fg} \right)$$

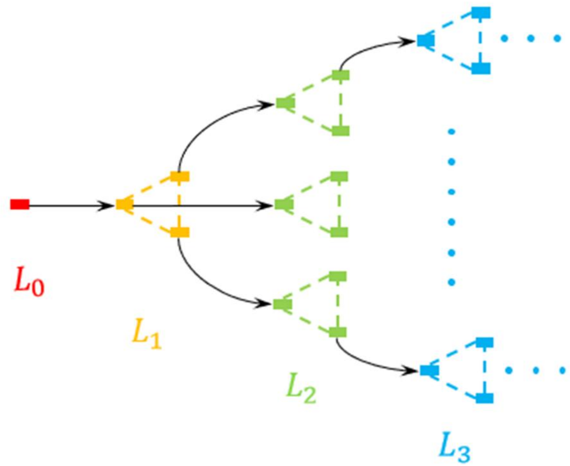

Afterwards, reject outlier correspondences by the Mahalanobis distance, and Initialize the 3D plane feature with measurements across multiple frames.

Observability Analysis of the LiDAR-IMU Subsystem

- The state vector of the LiDAR-IMU subsystem and state observability matrix

$$\mathbf{x} = \begin{bmatrix} \mathbf{x}_I^\top & \mathbf{x}_{\text{calib\_}L}^\top & {}^G\mathbf{p}_\pi^\top \end{bmatrix}^T$$

$$\mathbf{M}_k = \mathbf{H}_\pi \begin{bmatrix} L\mathbf{R}_G^I \widehat{\mathbf{R}} \mathbf{0}_{3\times1} \\ \mathbf{0}_1^\mathbf{I}\mathbf{1} \end{bmatrix} \times \begin{bmatrix} \Gamma_{\pi 11} & \mathbf{0}_3 & \mathbf{0}_3 & \Gamma_{\pi 14} & \mathbf{0}_3 & \Gamma_{\pi 16} & \mathbf{0}_3 & \Gamma_{\pi 18} & \Gamma_{\pi 19} \\ \Gamma_{\pi 21} & \mathbf{G}^\top & \mathbf{G}_\mathbf{n}^\top \Delta t_k & \Gamma_{\pi 24} & \Gamma_{\pi 25} & \Gamma_{\pi 26} & \Gamma_{\pi 27} & \Gamma_{\pi 28} & \Gamma_{\pi 29} \end{bmatrix}$$

TABLE I: Summary of degenerate motions for LiDAR-IMU calibration with one-plane feature.

One Plane / Parallel Planes	Unobservable
Pure Translation	${}_I^L\mathbf{R}$, ${}^L\mathbf{p}_I$
1-axis Rotation	${}^L\mathbf{p}_I$ along rotation axis
Constant ${}^I\omega$ and ${}^I\mathbf{v}$	t_{dL}, ${}^L\mathbf{p}_I$
Constant ${}^I\omega$ and ${}^G\mathbf{a}$	t_{dL}, ${}^L\mathbf{p}_I$
${}^G\boldsymbol{\omega} \parallel {}^G\mathbf{n}$ and ${}^G\mathbf{n} \perp {}^G\mathbf{v}$	t_{dL}

Experiments: Simulation

- Simulation inside a synthetic room with plane structures

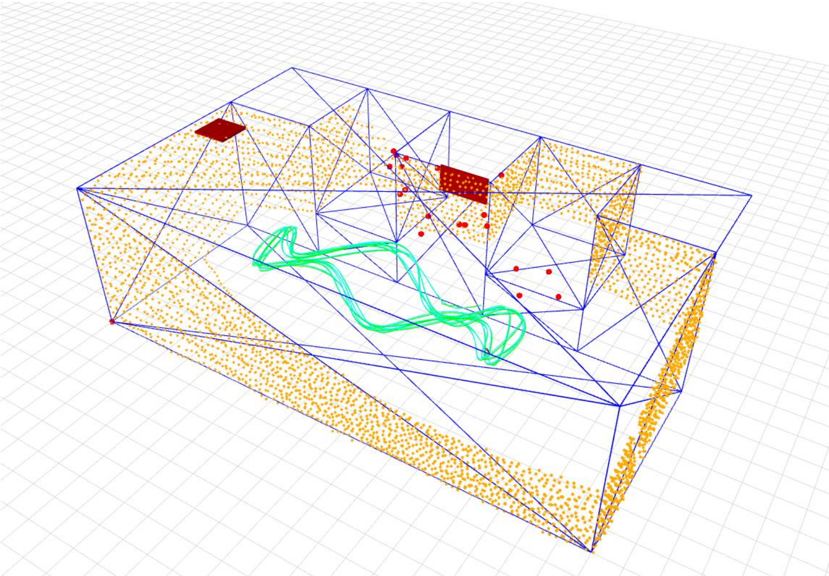

Table. The ATE and NEES of over 12 simulations under different setups of perturbation to initial values and online calibration.

IMU Model	ATE (deg)	ATE (m)	Ori. NEES	Pos. NEES
true w/ calib	0.118	0.020	2.210	0.185
bad w/ calib	0.129	0.021	2.216	0.221
bad w/o calib	0.148	0.024	2.677	0.246
true w/o calib	0.122	0.021	2.233	0.208
IC true w/o calib	0.159	0.027	2.237	0.314

The results demonstrates the consistency of the whole estimator with LiDAR, IMU and camera measurements!

Experiments: Simulation – Convergence of LiDAR-IMU Intrinsics

- Under random motion

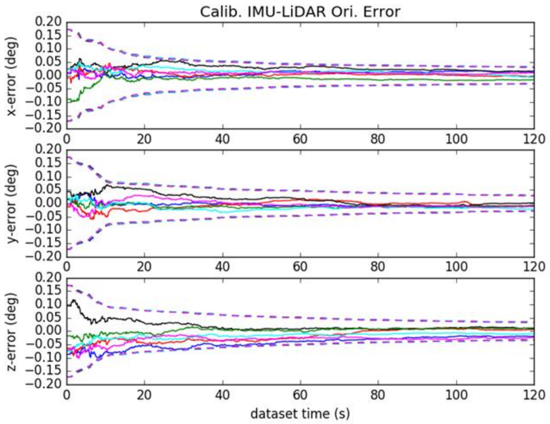

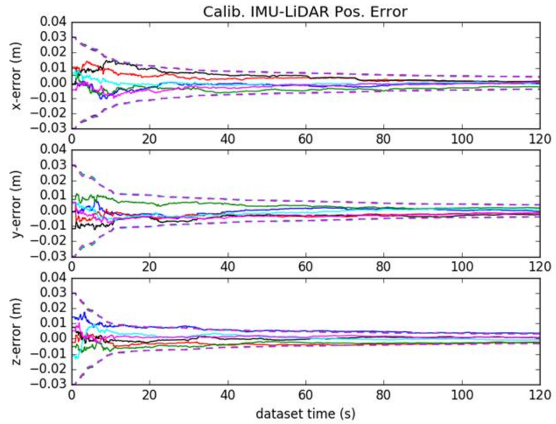

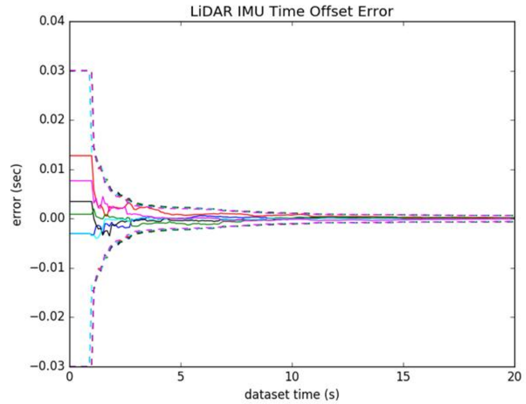

- Under degenerate motion of 1-axis rotation motion around yaw

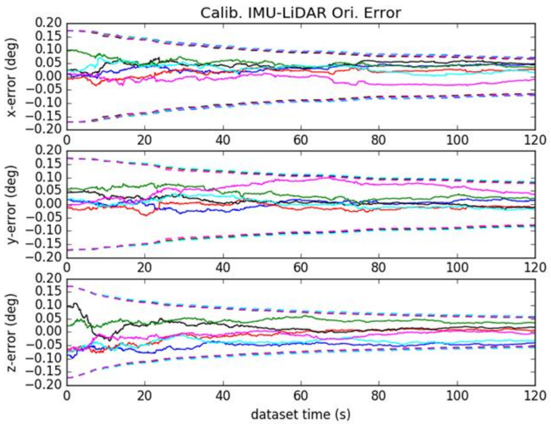

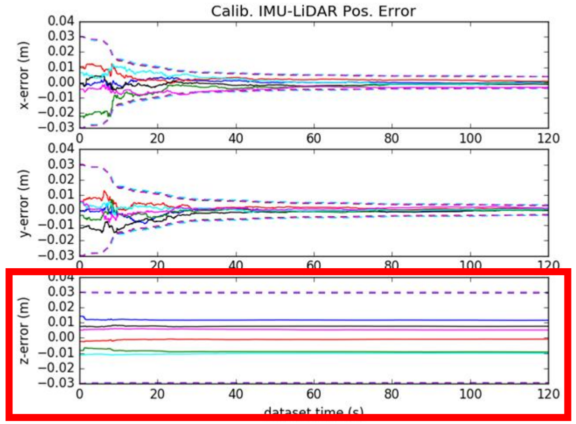

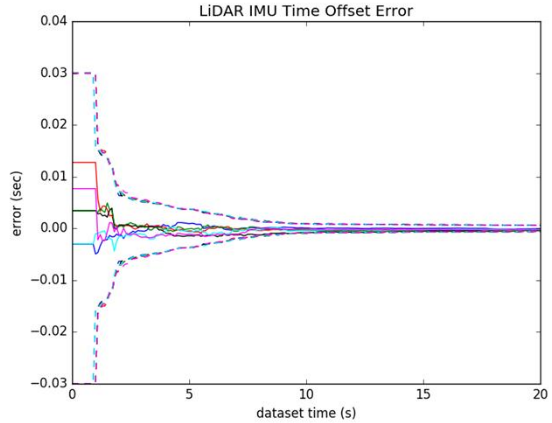

Experiments: Real-world, Teach Building Scenario

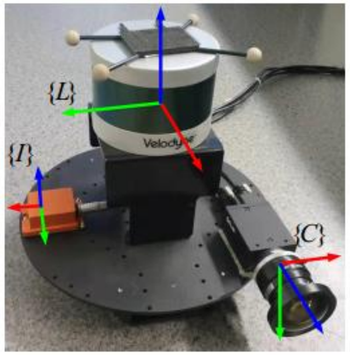

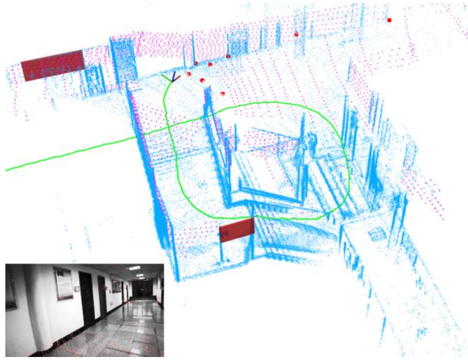

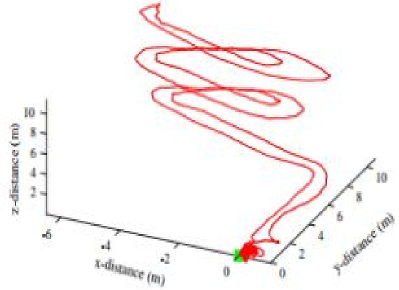

TABLE V: Averaged Start-to-End drift Error of 5 runs on Teaching Building Sequences (unit meters). The lengths for Seq1 - Seq 7 are around 108, 124, 237, 195, 85, 140, 83 meters, respectively. Note that estimated trajectories on Seq 1 and 2 are shown in Fig. 5.

Methods	Seq 1	Seq 2	Seq 3	Seq 4	Seq 5	Seq 6	seq7
LIC-Fusion 2.0	0.213, 0.074, 0.338	0.136, -0.107, -0.140	**0.689, -0.404, -0.172**	**0.456, 0.122, -0.322**	**0.054, -0.168, -0.027**	**0.025, -0.654, 0.199**	1.911, 0.226, -0.166
OpenVINS-IC	-, -, -	-1.765,-1.149,-0.836	3.917, 3.552, -0.475	3.181, -0.595, -1.372	-1.093,-0.083,-0.362	-0.085,-3.223,-0.143	-2.312, 1.562, 0.247
Proposed-LI	0.401, -0.195, 0.655	0.203, 0.503, 0.037	-, -, -	0.164,22.251,0.502	1.542, -2.110, 0.342	-, -, -	1.242, -0.462, -0.530
LOAM	0.831, -5.145, -0.607	**-0.059, -0.065, 0.073**	-3.418, 3.938, -21.364	-0.933, -8.395, 0.098	-9.014, 1.084, -0.300	-0.130, 0.461, 2.960	1.612, 0.000, -2.867
LIO-MAP	**-0.104, 0.057, 0.092**	-0.019, -0.423, 0.223	-, -, -	0.471, -0.215, -1.37	0.147, 0.017, -0.232	0.206, 0.125, 1.530	**0.019, -0.039, -0.142**
LIC-Fusion	-0.740, 0.0401, 0.222	0.293, 0.984, -0.656	1.216, 1.831, -0.465	-1.117, 0.607, 0.529	-0.382, -2.248, -0.905	-3.295, -1.934, 0.585	-0.912, -0.847, 0.377

Experiments: Real-world, Teach Building Scenario

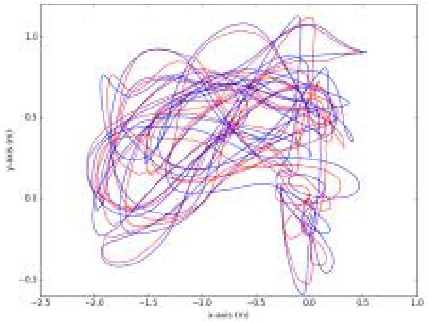

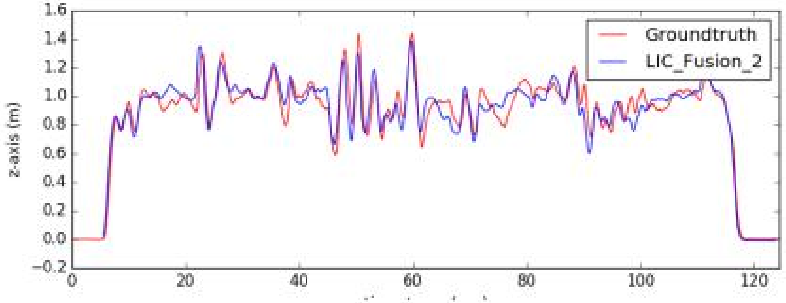

TABLE VI: Averaged ATE of 5 runs on Vicon Room Sequences (units degrees/meters). The lengths for Seq 1 - Seq 6 are 42.62, 84.16, 33.92, 53.14, 49.74, 87.87 meters, respectively. Note that estimated trajectory on Seq 2 is shown in Fig. 5

Methods	**Seq 1**	**Seq 2**	**Seq 3**	**Seq 4**	**Seq 5**	**Seq 6**	**Average**
LIC-Fusion 2.0	2.537 / 0.097	1.870 / 0.145	**1.940** / **0.101**	**2.081** / 0.116	**2.710** / 0.104	**3.320** / **0.113**	**2.410** / **0.113**
OpenVINS-IC	2.625 / **0.094**	**1.741** / 0.177	3.131 / 0.273	2.404 / **0.115**	2.962 / 0.129	3.953 / 0.129	2.803 / 0.153
Proposed-LI	2.333 / 0.199	3.325 / 0.444	2.810 / 0.306	5.335 / 0.272	3.332 / 0.440	4.866 / 0.412	3.667 / 0.345
LOAM	5.880 / 0.156	6.414 / **0.134**	15.384 / 0.333	6.354 / 0.150	5.542 / 0.140	7.095 / 0.188	7.778 / 0.183
LIO-MAP	- / -	5.608 / 0.214	- / -	- / -	4.890 / 0.170	12.862 / 0.238	7.786 / 0.207
LIC-Fusion	**2.345** / 0.097	1.879 / 0.173	1.973 / 0.104	- / -	2.743 / **0.100**	3.788 / 0.131	2.546 / 0.121

System Demonstration: Simulation

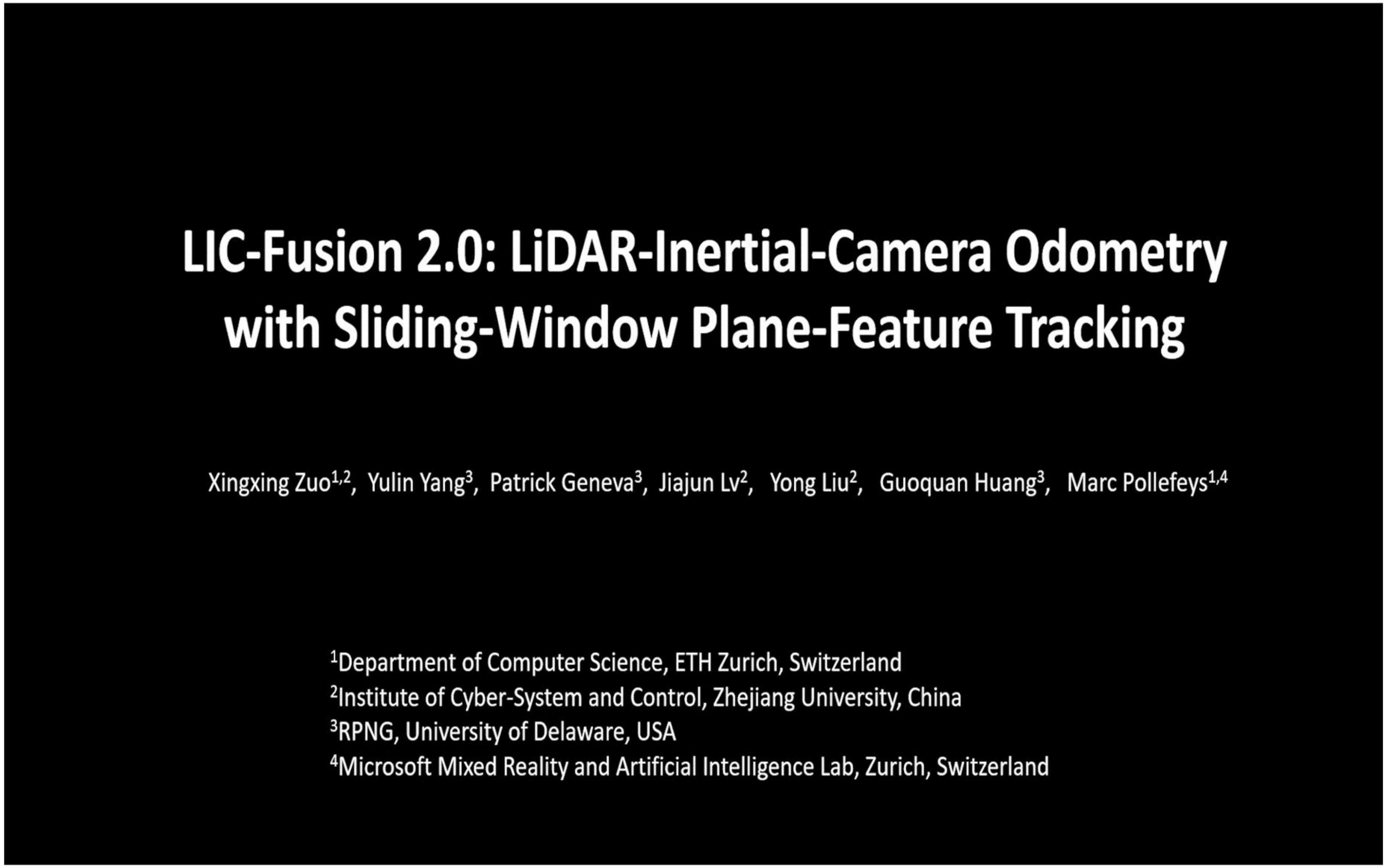

System Demonstration: Simulation

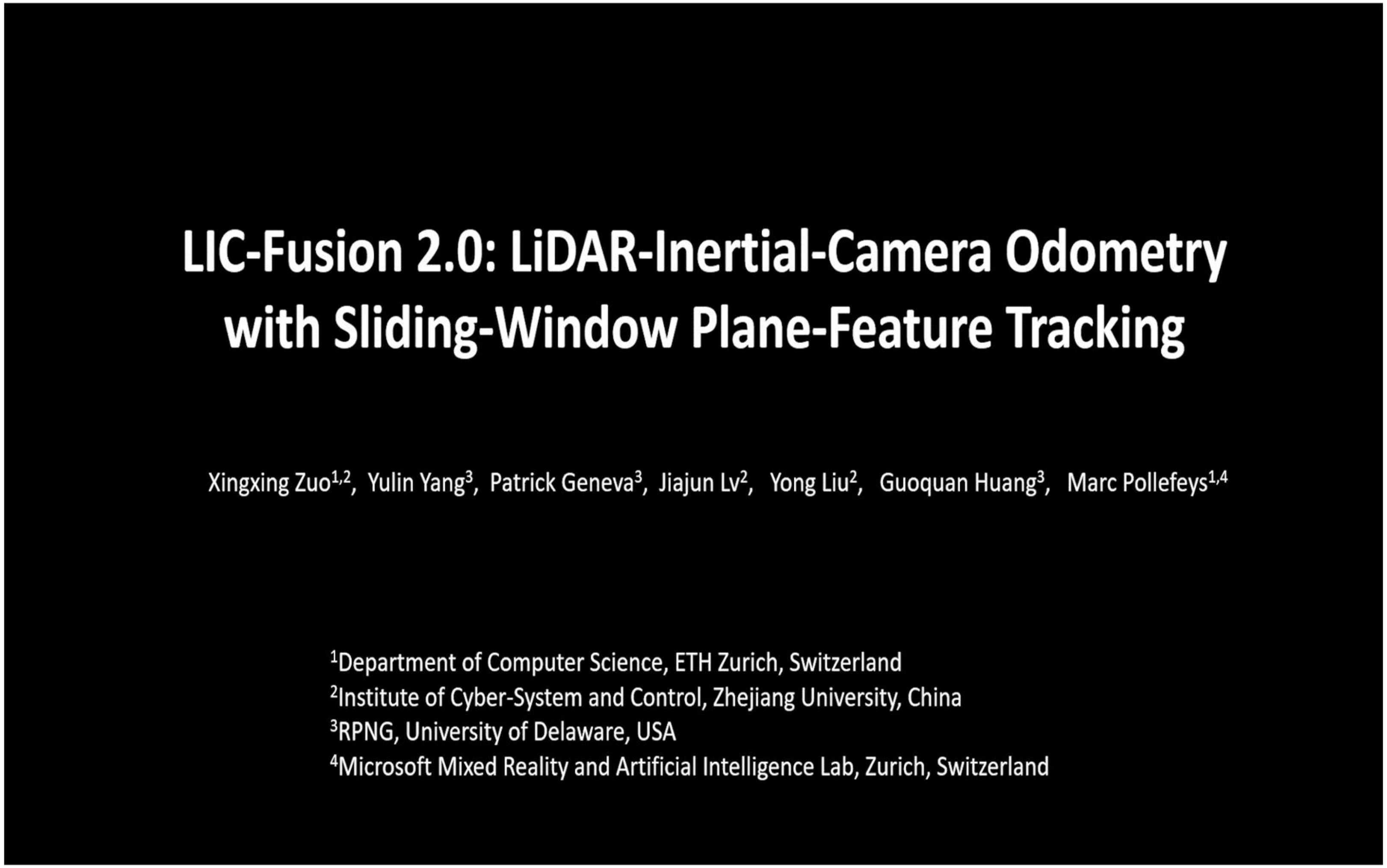

Conclusion

- Propose a plane-feature tracking method for 3D LiDAR, and advocate a new outlier rejection criterion to improve feature matching quality by taking to account the uncertainty of relative pose.

- Efficient and consistent tightly-coupled LiDAR-inertial-camera odometry without inconsistency-prone ICP based LiDAR scan matching.

- In-depth observability analysis of the LiDAR-inertial subsystem with plane features and identify the degenerate cases.

- Verified on both simulation and real-world experiments, and demonstrated to outperform the state-of-the-art by fusing measurements in a stochastic way.

Thanks for listening!

Happy to answer your questions!

Xingxing Zuo
xinzuo@ethz.ch

Computer Vision and Geometry Lab

APRIL机器人智能感知与学习实验室
Advanced Perception on Robotics and Intelligent Learning Lab

RPNG

References

1. X. Zuo, P. Geneva, W. Lee, Y. Liu, and G. Huang. “LIC-Fusion: LiDAR-Inertial-Camera Odometry”. In: Proc. IEEE/RSJ International Conference on Intelligent Robots and Systems (IROS). Nov. 2019, pp. 5848–5854.
2. J. Zhang, S. Singh, LOAM: Lidar Odometry and Mapping in Real-time[C], Robotics: Science and Systems. 2014, 2: 9.
3. P. Geneva, K. Eckenhoff, W. Lee, Y. Yang, and G. Huang. “OpenVINS: A Research Platform for Visual-Inertial Estimation”. In: Proc. of the IEEE International Conference on Robotics andAutomation (ICRA). Paris, France, 2020.
4. J. Zhang and S. Singh. “Laser–visual–inertial odometry and mapping with high robustness and low drift”. In: Journal of Field Robotics 35.8 (2018), pp. 1242–1264.
5. A. I. Mourikis and S. I. Roumeliotis, “A multi-state constraint Kalman filter for vision-aided inertial navigation,” in Proc. IEEE Int. Conf. Robot. Autom., Rome, Italy, Apr. 10–14, 2007, pp. 3565–3572.
6. H. Ye, Y. Chen, and M. Liu. “Tightly coupled 3d lidar inertial odometry and mapping”. In: 2019 International Conference on Robotics and Automation (ICRA). IEEE. 2019, pp. 3144–3150.
7. Y. Yang, P. Geneva, K. Eckenhoff, and G. Huang. “Degenerate motion analysis for aided ins with online spatial and temporal sensor calibration”. In: IEEE Robotics and Automation Letters 4.2 (2019), pp. 2070–2077.

Contributions

- A novel sliding-window plane-feature tracking algorithm that allows data association across multiple LiDAR scans, and a probabilistic outlier rejection criterion. Improving the data association in our prior tightly-coupled fusion framework: LIC-Fusion

- In-depth observability analysis of the LiDAR-inertial-camera system with plane features and identify the degenerate cases.

- A consistent estimator fusing IMU measurements, sparse visual features, and sparse LiDAR features in a light-weight EKF based framework.

- Validate proposed system in both simulated and real-world dataset, and the proposed shows superior performance over the state-of-the-art regarding accuracy and is verified to be consistent.